Received: 3 April 2024 | Revised: 29 July 2024 | Accepted: 6 August 2024

DOI: 10.1002/dta.3791

RESEARCH ARTICLE

WILEY

Human phase-I metabolism of three synthetic cannabinoids bearing a cumyl moiety and a cyclobutyl methyl or norbornyl methyl tail: Cumyl-CBMEGACLONE, Cumyl-NBMEGACLONE, and Cumyl-NBMINACA

Arianna Giorgetti[1,2] | Pietro Brunetti[2,3] | Belal Haschimi[2] | Benedikt Pulver[2] | Jennifer Paola Pascali[1] | Jan Riedel[4] | Volker Auwärter[2]

[1]Department of Medical and Surgical Sciences, Unit of Legal Medicine, University of Bologna, Bologna, Italy

[2]Institute of Forensic Medicine, Forensic Toxicology, Medical Center – University of Freiburg, Faculty of Medicine, University of Freiburg, Freiburg im Breisgau, Germany

[3]Pharmaceutical Sciences, Roche Pharma Research and Early Development, Roche Innovation Center Basel, Basel, Switzerland

[4]Federal Criminal Police Office, Forensic Science Institute, Wiesbaden, Germany

Correspondence
Arianna Giorgetti, Department of Medical and Surgical Sciences, Unit of Legal Medicine, University of Bologna, Via Irnerio 49, Bologna 40126, Italy.
Email: arianna.giorgetti@unibo.it; ari.giorgetti@gmail.com

Abstract

Synthetic cannabinoid receptor agonists (SCRAs) continue to show high prevalence on the new psychoactive substances drug market. Around 2019–2020, new SCRAs bearing a cumyl moiety emerged: Cumyl-CBMEGACLONE and Cumyl-NBMEGACLONE, carrying a cyclobutyl methyl (CBM) and a norbornyl methyl moiety (NBM) attached to the γ-carbolinone core. These were followed by Cumyl-NBMINACA, the indazole carboxamide analog of Cumyl-NBMEGACLONE. The study aimed at evaluating the human phase-I metabolism of these compounds and at identifying suitable urinary markers to prove their consumption. After enzymatic hydrolysis, 14 authentic urine samples (eight for Cumyl-CBMEGACLONE, four for Cumyl-NBMEGACLONE, and two for Cumyl-NBMINACA) were analyzed by liquid chromatography–quadrupole time-of-flight mass spectrometry. Results were compared with in vitro metabolites generated by pooled human liver microsomes incubation. Fifteen human phase-I metabolites were identified for Cumyl-CBMEGACLONE, nine for Cumyl-NBMEGACLONE, and thirteen for Cumyl-NBMINACA. The main in vivo metabolites were built by monohydroxylation, dihydroxylation, or trihydroxylation. The following urinary biomarkers are suggested for detecting the consumption of the investigated SCRAs: products of monohydroxylation at the CBM and at the core for Cumyl-CBMEGACLONE; two products of monohydroxylation at the norbonyl methyl tail for Cumyl-NBMEGACLONE; and metabolites built by dihydroxylation at the NBM substructure and by an additional hydroxylation at the cumyl moiety for Cumyl-NBMINACA.

KEYWORDS
forensic toxicology, mass spectrometry, metabolism study, new psychoactive substances, synthetic cannabinoids

1 | INTRODUCTION

Synthetic cannabinoid receptor agonists (SCRAs) represent one of the largest and continuously growing groups among the new psychoactive substances (NPS). According to the European Monitoring Centre for Drugs and Drug Addiction, recently renamed as the European Union Drugs Agency, more than 245 SCRAs have been monitored so far.[1] SCRAs were first detected in herbal material around 2008,[2] and since then, several new compounds with structural modifications have been introduced on the NPS market.

The dynamic market of SCRAs reflects a cat-and-mouse game between NPS manufacturers and legislation that strives to include novel compounds, either on a substance-by-substance basis or by generic definitions. The scheduling of compounds inevitably fuels the production of new, legal molecules and leads to the invention of novel structures and substructures.[3] Prompted by national and international regulations, indeed, clandestine laboratories began synthetizing SCRAs characterized by entirely new chemical substructures, some of which include a cumyl moiety. This cumyl substituent was described in a patent application for "SGT compounds,"[4] where it was attached to an indole, indazole, or azaindole core structure.

The first cumyl-containing SCRA bearing a γ-carbolinone core structure (5-pentyl-2-(2-phenylpropan-2-yl)-2,5-dihydro-1*H*-pyrido[4,3-*b*]indol-1-one, with the semisystematic name Cumyl-PEGACLONE or SGT-151) emerged on the NPS market and was first analytically characterized around 2016.[5–7] The compound soon dominated the German SCRA market, being detected in about 25% of the herbal blends monitored at the University of Freiburg and was also connected to a high number of allegedly "benign" intoxications.[6,8] In 2018, following the success of Cumyl-PEGACLONE, the 5-fluoropentyl analog 5-(5-fluoropentyl)-2-(1-methyl-1-phenylethyl)-1*H*-pyrido[4,3-b]indol-1-one (semisystematic name: Cumyl-5F-PEGACLONE) emerged and was linked to several death cases.[9,10]

In September 2018, a new γ-carbolinone-derived SCRA bearing a cyclohexyl methyl group at the core structure was named Cumyl-CHMEGACLONE (5-cyclohexylmethyl-2-(2-phenylpropan-2-yl)-2,5-dihydro-1*H*-pyrido[4,3-*b*]indol-1-one).[11] Due to the growing number of compounds featuring this substructure and the health risks associated with the use of the corresponding SCRAs, in 2019, the German generic law for controlling groups of NPS based on their chemical structures (NpSG) was updated to include the γ-carbolinone core in the structural definitions for SCRAs.[12]

Around 2019–2020, the amendment of the NpSG likely resulted in a shift toward the production of SCRAs containing a new tail group, namely, the cyclobutyl methyl (CBM) moiety. This led to the emergence of Cumyl-CBMICA, rapidly followed by its indazole counterpart Cumyl-CBMINACA and by Cumyl-CBMEGACLONE (5-(cyclobutylmethyl)-2-(1-methyl-1-phenyl-ethyl)pyrido[4,3-*b*]indole-1-one), the CBM analog of Cumyl-PEGACLONE.[13,14]

The latest generation of SCRAs with the cumyl moiety appeared on the market more recently, featuring a structural modification of the side chain. Specifically, a bicyclic, saturated hydrocarbon side chain was introduced and used to synthesize compounds with varying core structures.[15] This norbornyl methyl (NBM) tail structure is carried by 5-(bicyclo[2.2.1]hept-2-yl)methyl)-2-(2-phenylpropan-2-yl)-2,5-dihydro-1*H*-pyrido[4,3-*b*]indol-1-one (semisystematic name: Cumyl-NBMEGACLONE or Cumyl-BC[2.2.1]HpMeGaClone), a γ-carbolinone SCRA, and by 1-(bicyclo[2.2.1]heptan-2-yl)methyl)-*N*-(2-phenylpropan-2-yl)-1*H*-indazole-3-carboxamide (semisystematic name: Cumyl-NBMINACA).[14] So far, the metabolism of these compounds has not yet been elucidated.

In Figure 1, some of the SCRAs bearing a cumyl, a CBM, and/or a NBM moiety are shown.

All these compounds have been recently characterized for their affinity and potency at the human cannabinoid receptor 1, showing full agonist properties with varying potencies. Particularly, Cumyl-CBMEGACLONE exhibited higher affinity and potency compared with Cumyl-CBMICA and Cumyl-CBMINACA. Moreover, the NBM side chain seems to further increase affinities and potencies.[16]

Because the metabolism of these compounds has not yet been elucidated, the present study aimed to investigate the human phase-I metabolism of Cumyl-CBMEGACLONE, Cumyl-NBMEGACLONE, and

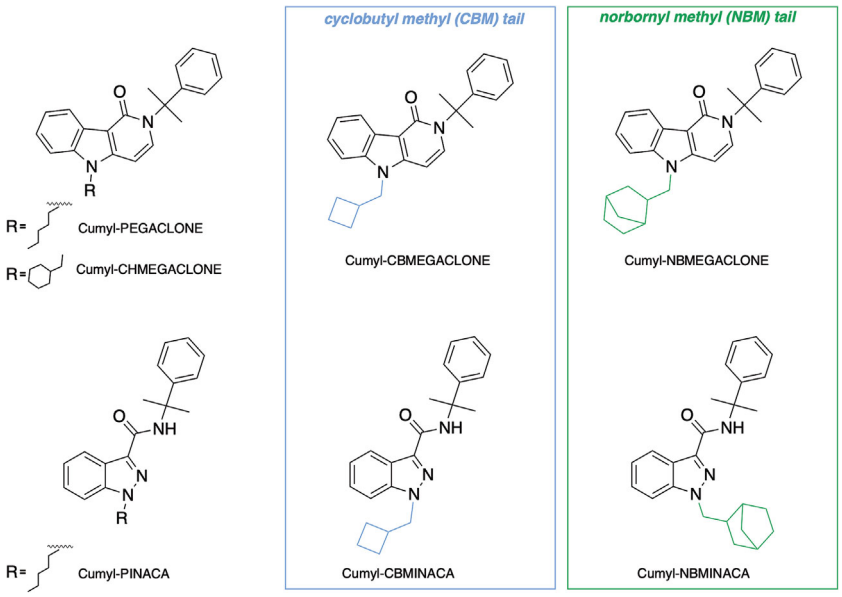

FIGURE 1 Chemical structures and semisystematic names of Cumyl-CBMEGACLONE, Cumyl-NBMEGACLONE, and Cumyl-NBMINACA and some of the structurally related mentioned synthetic cannabinoid receptor agonists.

Cumyl-NBMINACA and to compare the metabolites detected with those generated in vitro, in order to identify urinary biomarkers useful as unequivocal proof of their consumption.

2 | MATERIAL AND METHODS

2.1 | Chemicals and reagents

Formic acid (Rotipuran® ≥ 98%, p.a.), sodium hydroxide (≥99%, p.a., pellets), and potassium hydrogen phosphate (≥99%, p.a.) were obtained from Carl Roth (Karlsruhe, Germany). Acetonitrile (ACN) (LC–MS grade) and ammonium formate 10 M (99.995%) were bought from Sigma Aldrich (Steinheim, Germany). Isopropanol (Prepsolv®) was obtained from Merck (Darmstadt, Germany). Acetic acid glacial (USP, EP, and JP grades) was purchased from VWR (Darmstadt, Germany). Pooled human liver microsomes (pHLMs; 50 donors, 20 mg/mL protein in 250 mM sucrose), NADPH-regenerating Solutions A and B (reductase activity 0.43 μmol/min * ml), and potassium phosphate buffer 0.5 M (pH 7.4) were purchased from Corning (New York, USA). NADPH-regenerating Solution A consisted of 26 mM $NADP^+$, 66 mM glucose-6-phosphate, and 66 mM $MgCl_2$ in water. NADPH-regenerating Solution B consisted of 40 U/mL glucose-6-phosphate dehydrogenase in 5 mM sodium citrate. Roche Diagnostics (Mannheim, Germany) produced the β-glucuronidase (*Escherichia coli* K12) used for conjugate cleavage.

The reference standard for Cumyl-CBMEGACLONE was purchased from Cayman Chemical (Ann Arbor, MI, USA), while Cumyl-NBMEGACLONE and Cumyl-NBMINACA were provided as purified standards isolated from herbal blend material, as described elsewhere,[17] within the framework of the EU-project ADEBAR *plus*.[18] Analytical data on the latter two can be found in Figures S1 and S2 and Tables S1 and S2.

Deionized water was prepared using a Medica® Pro deionizer from ELGA (Celle, Germany). Blank urine samples were donated by a volunteer and tested for the absence of SCRAs' metabolites prior to its use. Mobile phase A (1% ACN, 0.1% HCOOH, and 2 mM NH_4^+ $HCOO^-$ in water) and mobile phase B (0.1% HCOOH and 2 mM NH_4^+ $HCOO^-$ in ACN) were freshly prepared prior to analysis. The sodium formate/acetate clusters solution used for external and internal mass calibration of the qToF-MS instrument was prepared by mixing 250 mL deionized water, 250 mL isopropanol, 750 μL acetic acid, 250 μL formic acid, and 500 μL sodium hydroxide 1 M.

2.2 | Authentic human urine samples and preparation

For identification of the in vivo phase-I main metabolites of Cumyl-CBMEGACLONE, Cumyl-NBMEGACLONE, and Cumyl-NBMINACA, the liquid chromatography–quadrupole time-of-flight mass spectrometry (LC-qToF-MS) analysis was performed with eight, four, and two urine samples, obtained from 14 different individuals. Urine samples were sent around 2020–2021 for SCRAs testing to the Forensic Toxicology department in Freiburg, Germany, and were mostly provided by forensic psychiatric hospitals from various regions in Germany or by German prisons. All analyses were conducted in accordance with the inquiry of the respective client (abstinence control): urine samples were screened by an LC–MS/MS method that monitors the metabolites of the most prevalent SCRAs. Urine samples were then selected for the present study when tested positive for the anticipated metabolites of Cumyl-CBMEGACLONE, Cumyl-NBMEGACLONE, or Cumyl-NBMINACA, based on typical metabolic reactions observed for structurally similar compounds.

Preparation of specimens was performed as in previously published methods.[19] Briefly, a volume of 0.5 mL of phosphate buffer and 30 μL β-glucuronidase were added to 0.5 mL of urine. A 1 h incubation at 45°C was performed and quenched by addition of 1.5 mL ice-cold ACN; then, 0.5 mL of a 10 M ammonium formate solution were added. The mixture was shaken (overhead mixing) for 5 min and centrifuged for 10 min at 2900*g* (Heraeus Megafuge 1.0, Thermo Scientific, Schwerte, Germany). Then, 1 mL of the organic layer was transferred into a separate vial and evaporated to dryness under a stream of nitrogen. Finally, the samples were reconstituted in 25 μL mobile phase A/B (50/50, v/v) prior to LC-qToF-MS analysis (Section 2.4). Negative control samples (blank urine) were prepared accordingly.

2.3 | pHLM assay

In vitro phase-I metabolites of Cumyl-CBMEGACLONE, Cumyl-NBMEGACLONE, and Cumyl-NBMINACA were generated by applying a pHLM assay. The in vitro assay was performed by adding 0.5 μL of an ACN-based 1 mg/mL reference standard solution (final concentration of 10 μg/mL in incubation mixture) to 49.5 μL of a reaction mixture consisting of 2.5 μL pHLM, 2.5 μL NADPH-regenerating Solution A, 0.5 μL NADPH-regenerating Solution B, 10 μL phosphate buffer 0.5 M (pH 7.4), and 34 μL deionized water. The reaction was performed during a 30 min incubation at 37°C and was terminated by the addition of 150 μL ice-cold ACN. After the addition of 25 μL of a 10 M ammonium formate solution, the sample was centrifuged for 4 min at 13,000 rpm (16,060*g*). Then, the organic layer was transferred into a separate vial. For LC-qToF-MS analysis (parameters described in Section 2.4), 30 μL of the extracts were evaporated to dryness under a stream of nitrogen and reconstituted in 30 μL mobile phase A/B (50/50, v/v). Two blank pHLM samples, one containing no reference standard (zero control) and the other one containing no pHLM enzymes (blank control), were processed accordingly and served as negative controls. The experiments were performed in triplicates.

2.4 | Instrumentation and identification of tentative main metabolites (LC-qToF-MS)

To identify the main in vivo and in vivo metabolites, LC-qToF-MS analysis of urine samples and pHLM incubates was performed on an

Impact II QToF instrument coupled with an Elute HPLC system (Bruker Daltonik, Bremen, Germany). Chromatographic separation was performed on a Kinetex® C18 column (2.6 µm, 100 Å, 100 × 2.1 mm; Phenomenex, Aschaffenburg, Germany) applying gradient elution as follows: starting condition of mobile phase B was 20%, linearly increased to 50% in 8.0 min, further increased to 60% in 2.0 min, further increased to 95% in 2.0 min, held for 1.0 min, decreased to starting conditions of 20% in 0.1 min, and held for 2.9 min for re-equilibration, resulting in a total run time of 15 min. The flow rate was set to 0.5 mL/min. Autosampler and column oven temperatures were set to 10°C and 40°C, respectively. The injection volume was 5 µL. HyStarTM ver. 3.2 and DataAnalysis ver. 4.2 (Bruker Daltonik, Bremen, Germany) were used for data acquisition and processing, respectively. The MS was operated in positive electrospray ionization mode acquiring spectra in the *m/z* range of 50 to 650 for each scan and mode. The dry gas temperature was set to 200°C with a dry gas flow of 8.0 L/min. The nebulizer gas pressure was 2 bar. Nitrogen was used as collision gas. The voltages for the capillary and end plate offset were 2500 and 500 V, respectively. External and internal mass calibrations were performed using sodium formate/acetate clusters and high-precision calibration mode.

In a first run, full scan and broadband collision-induced dissociation data (collision energy 35 ± 7 eV) were acquired to screen for metabolites at an acquisition rate of 2.0 Hz. The resulting spectra were compared with a list of hypothetical metabolites, based on the known biotransformations of structurally similar SCRAs, for example, monohydroxylation, dihydroxylation, and trihydroxylation; ketone formation; dehydrogenation; *N*-dealkylation (tail); *N*-decumylation; and dihydrodiol formation, as well as combinations thereof.

The resulting hits for the molecular ions of anticipated metabolites were further analyzed by auto-MS/MS for pHLM (with a maximum of three MS–MS cycles performed on each precursor ion) to record product ion spectra.

Furthermore, precursor ion analysis of the data obtained from full scan and broadband collision-induced dissociation data mode was performed with characteristic fragment ions (particularly *m/z* 185.0709 for Cumyl-CBMEGACLONE and Cumyl-NBMEGACLONE and *m/z* 145.0396 for Cumyl-NBMINACA) to detect unexpected metabolites not covered by the inclusion list.

The following criteria were applied for metabolite identification: mass error of the precursor ion <5 ppm, a signal-to-noise ratio >3:1, and a mass tolerance for fragment ions of ±10 ppm.

In vitro metabolites generated by pHLM incubation were used for confirmation in the sense of plausibility control. For this purpose, for each metabolite detected in an authentic human urine sample, retention times (±0.1) and protonated masses as well as masses of at least two fragment ions were compared with the values obtained from analysis of the pHLM incubates.

For comparison of the relative metabolic profiles, the following procedure was applied. (I) For each detected metabolite in a urine sample, peak area ratios were calculated by dividing the peak area of the metabolite by the peak area of the most abundant metabolite within the sample, which was further set to 100%. (II) Then, for each metabolite, a mean area ratio (MAR%) was calculated as the average of the peak area ratio across all analyzed authentic urine samples. (III) Lastly, metabolites were assigned a ranking position on the basis of the MAR%, with upper ranking for the bigger MAR% values and lower ranking for the smaller MAR% values.

Target urinary biomarkers for screening SCRA consumption were selected on the basis of the specificity, that is, metabolites not produced by structurally related SCRAs, and abundancy, selecting those with higher MAR%.

3 | RESULTS AND DISCUSSION

3.1 | Cumyl-CBMEGACLONE

The unchanged Cumyl-CBMEGACLONE ($[M + H]^+$ at *m/z* 371.2118) was not detected in any authentic urine specimens, not even in highly concentrated ones, in contrast to the structurally similar Cumyl-CHMEGACLONE.[11] Under the used chromatographic conditions, Cumyl-CBMEGACLONE eluted at 10.5 min and was detected in the blank control as well as in the pHLM assays. Characteristic ion fragments were seen at *m/z* 253.1335, corresponding to the CBM attached to the core, further fragmented to *m/z* 225.1022 (opening of the cyclobutane ring), at *m/z* 185.0709 and at *m/z* 167.0604, both corresponding to the γ-carbolinone core, and at *m/z* 119.0855 (dimethylbenzyl cation). A fragment corresponding to the tail, at *m/z* 69.0699, could also be detected, though with lower intensity.

Fifteen metabolites were detected by the analysis of authentic urine specimens after enzymatic cleavage of glucuronides. These were assigned to the following biotransformations: monohydroxylation and dihydroxylation, as well as *N*-dealkylation and *N*-decumylation combined with monohydroxylation or dihydroxylation (Table 1). In Table 1, the MAR% of the metabolites is also shown. In Figure 2, the fragmentation pattern of Cumyl-CBMEGACLONE and of its metabolites, as detected in authentic urine samples, is shown.

The most abundant product was M13, detected with $[M + H]^+$ at *m/z* 387.2067. Diagnostic product ions were seen at *m/z* 185.0709, corresponding to the intact γ-carbolinone core, coupled to a fragment ion at *m/z* 269.1285 (+15.9950 u) with respect to the fragment at *m/z* 253.1335, suggesting that a monohydroxylation took place at the CBM tail. In the case of M13, further fragments were detected at *m/z* 167.0604, *m/z* 251.1179, and *m/z* 233.1073, which could be formed by the loss of water molecules from the core and/or from the CBM. Similar fragments were also seen in the corresponding in vitro-generated metabolites and suggest that monohydroxylation did not occur at an aromatic structure, confirming the hypothesis of hydroxylation at the CBM tail.

Moreover, the sodium adduct at *m/z* 409.1886 and the fragment corresponding to the cumyl moiety at *m/z* 119.0855 were identified. M12 shared the same protonated mass and fragments, but with far less abundance.

TABLE 1 Cumyl-CBMEGACLONE human phase-I metabolites detected by liquid chromatography–quadrupole time-of-flight mass spectrometry analysis of eight urine samples.

ID	RT (min)	Biotransformation	Ranking position	MAR in vivo (% and (*SD*))	Number of positive samples	Calculated $[M+H]^+$	Formula $[M+H]^+$	Mass error (ppm)	Diagnostic product ions calc. (*m/z*)	Diagnostic product ions formula	Diagnostic product i ons mass error (ppm)	In vitro confirmation via pHLM
M00	10.5	–	–	–	–	371.2118	$C_{25}H_{27}N_2O^+$	−0.5	119.0855	$C_9H_{11}^+$	2.4	–
									185.0709	$C_{11}H_9N_2O^+$	1.8	
									253.1335	$C_{16}H_{17}N_2O^+$	2.1	
M1	1.2	*N*-decumylation + diOH (core, CBM)	7	7.1% (14.5)	3	285.1234	$C_{16}H_{17}N_2O_3^+$	0.2	201.0659	$C_{11}H_9N_2O_2^+$	−0.3	–
									183.0553	$C_{11}H_7N_2O^+$	−2.3	
M2	1.4	*N*-decumylation + diOH (core, CBM)	12	1.5% (1.5)	3	285.1234	$C_{16}H_{17}N_2O_3^+$	−0.2	201.0659	$C_{11}H_9N_2O_2^+$	0.2	–
									183.0553	$C_{11}H_7N_2O^+$	−0.1	
M3	3.6	*N*-decumylation + monoOH (core)	9	4.4% (7.3)	3	269.1285	$C_{16}H_{17}N_2O_2^+$	0.9	201.0659	$C_{11}H_9N_2O_2^+$	2.0	–
									183.0553	$C_{11}H_7N_2O^+$	0.7	
M4	3.9	*N*-dealkylation (CBM) + monoOH (core)	2	58.9% (39.2)	8	319.1441	$C_{20}H_{19}N_2O_2^+$	2.4	201.0659	$C_{11}H_9N_2O_2^+$	1.3	–
									119.0855	$C_9H_{11}^+$	1.7	
M5	4.0	*N*-dealkylation (CBM) + monoOH (core)	5	7.4% (7.3)	7	319.1441	$C_{20}H_{19}N_2O_2^+$	2.4	201.0659	$C_{11}H_9N_2O_2^+$	1.0	–
									119.0855	$C_9H_{11}^+$	0.9	
M6	4.3	*N*-dealkylation (CBM) + monoOH (core)	3	41.6% (23.7)	8	319.1441	$C_{20}H_{19}N_2O_2^+$	2.3	201.0659	$C_{11}H_9N_2O_2^+$	1.9	–
									119.0855	$C_9H_{11}^+$	1.6	
M7	4.6	*N*-decumylation + monoOH (core)	15	0.6% (1.5)	2	269.1285	$C_{16}H_{17}N_2O_2^+$	0.8	201.0659	$C_{11}H_9N_2O_2^+$	1.6	–
									183.0553	$C_{11}H_7N_2O^+$	1.4	
M8	4.7	DiOH (CBM, CBM)	13	0.8% (1.3)	4	403.2016	$C_{25}H_{27}N_2O_3^+$	1.3	285.1234	$C_{16}H_{17}N_2O_3^+$	0.6	✓
									185.0709	$C_{11}H_9N_2O^+$	0	
M9	5.1	DiOH (CBM, CBM)	11	1.8% (3.1)	5	403.2016	$C_{25}H_{27}N_2O_3^+$	−1.1	285.1234	$C_{16}H_{17}N_2O_3^+$	2.0	✓
									185.0709	$C_{11}H_9N_2O^+$	−0.2	
M10	5.2	DiOH (core, CBM)	6	7.2% (5.8)	7	403.2016	$C_{25}H_{27}N_2O_3^+$	1.4	285.1234	$C_{16}H_{17}N_2O_3^+$	1.9	✓
									201.0659	$C_{11}H_9N_2O_2^+$	−0.5	
M11	6.4	DiOH (core, CBM)	8	4.5% (3.5)	7	403.2016	$C_{25}H_{27}N_2O_3^+$	2.7	285.1234	$C_{16}H_{17}N_2O_3^+$	1.2	✓
									201.0659	$C_{11}H_9N_2O_2^+$	4.8	
M12	6.9	MonoOH (CBM)	14	0.7% (0.2)	4	387.2067	$C_{25}H_{27}N_2O_2^+$	1.2	269.1285	$C_{16}H_{17}N_2O_2^+$	0.4	✓
									185.0709	$C_{11}H_9N_2O^+$	−0.3	
M13	7.1	MonoOH (CBM)	1	100% (0)	8	387.2067	$C_{25}H_{27}N_2O_2^+$	1.2	269.1285	$C_{16}H_{17}N_2O_2^+$	2.1	✓
									185.0709	$C_{11}H_9N_2O^+$	1.7	
M14	8.1	MonoOH (core)	4	9.4% (4.4)	8	387.2067	$C_{25}H_{27}N_2O_2^+$	0.8	269.1285	$C_{16}H_{17}N_2O_2^+$	1.1	✓
									201.0659	$C_{11}H_9N_2O_2^+$	0.2	
M15	9.0	MonoOH (core)	10	3.6% (3.0)	7	387.2067	$C_{25}H_{27}N_2O_2^+$	−0.8	269.1285	$C_{16}H_{17}N_2O_2^+$	1.0	✓
									201.0659	$C_{11}H_9N_2O_2^+$	4.6	

Note: Ranking position is based on the mean MAR%, calculated in relation to the most abundant metabolite peak.

Abbreviations: CBM, cyclobutyl methyl tail; DiOH, dihydroxylation; MAR, mean area ratio; MonoOH, monohydroxylation; pHLM, pooled human liver microsomes; RT, retention time; *SD*, standard deviation.

M14 and M15 were characterized by a protonated mass at *m/z* 387.2067 and by fragment ions at *m/z* 269.1285 and at *m/z* 201.0659, pointing toward a monohydroxylation occurring at the γ-carbolinone core. A further fragment was seen at *m/z* 183.0553, which could correspond to the loss of water from the monohydroxylated γ-carbolinone core.[13]

Further hydroxylation could lead to M8–M11, identified by $[M + H]^+$ at *m/z* 403.2016. M8 and M9 were probably formed by dihydroxylation, both occurring at the CBM residue, yielding in diagnostic fragment ions at *m/z* 285.1234 and *m/z* 185.0709, corresponding to the unaltered core. Furthermore, the sodium adduct at *m/z* 425.1836 was noted. The corresponding in vitro metabolites also showed a fragment ion at *m/z* 269.1285 and at *m/z* 267.1128, the latter explained by loss of water from the fragment at *m/z* 285.1234.

M10 and M11 were characterized by a fragment ion at *m/z* 285.1234, at *m/z* 267.1128, due to the loss of water, and at *m/z* 201.0659, indicating a dihydroxylation involving once the core and once the CBM residue. Dihydroxylated products ranked from the sixth position to lower ranking scores.

At the second position among all authentic urine samples, with a MAR% of 58.9%, M4 was detected, which showed $[M + H]^+$ at *m/z* 319.1441, identical to M5 and M6. M4–M6 were characterized by fragment ions detected at *m/z* 201.0659, at *m/z* 183.0553 (loss of water), at *m/z* 119.0855 (loss of the cumyl moiety), and at *m/z* 341.1260 (the sodium adduct). This pattern is consistent with an *N*-dealkylation involving the CBM coupled to monohydroxylation at the core.

M3 and M7 shared the fragment ions at *m/z* 201.0659 and at *m/z* 183.0553 (due to the loss of water) but were also characterized by a fragment at *m/z* 291.1104 (sodium adduct) and showed a $[M + H]^+$ at *m/z* 269.1285, pointing toward an *N*-decumylation plus monohydroxylation of the core. Both were quite low in the ranking (9th and 15th positions, MAR% around 4.4% and 0.6%).

Lastly, at the 7th and 12th ranking positions, M1 and M2 were detected with a protonated mass ($[M + H]^+$) at *m/z* 285.1234, and characteristic fragment ions at *m/z* 201.0659, at *m/z* 183.0553, and at *m/z* 307.1053 (sodium adduct), allowing to hypothesize an *N*-decumylation plus a dihydroxylation, one occurring at the γ-carbolinone core and one at the CBM residue. However, these metabolites eluted in the front of the chromatograms only of highly concentrated samples, and in the absence of a pHLM-generated plausibility control, their structure can only be hypothesized.

In Supporting Information S1, the extracted ion chromatograms of one authentic urine sample (Figure S3) and of a pHLM assay (Figure S4) as well as the spectra of Cumyl-CBMEGACLONE metabolites as obtained from in vitro analysis are shown (Figure S5).

A product of *N*-dealkylation, not coupled to other reactions, could not be identified in vivo but only in vitro (Figure S5).

In vitro analysis confirmed 8 out of 15 in vivo detected metabolites. Particularly, none of the metabolites built by multiple biotransformations, for example, *N*-dealkylation or *N*-decumylation combined with monohydroxylation or dihydroxylation (M1–M7), could be confirmed by means of pHLM assay.

3.2 | Cumyl-NBMEGACLONE

As shown by the blank control and the pHLM assay, Cumyl-NBMEGACLONE ($[M + H]^+$ at *m/z* 411.2447) (M00) eluted at 11.7 min under the applied chromatographic conditions.

As already seen for Cumyl-CBMEGACLONE, characteristic fragments of Cumyl-NBMEGACLONE were detected at *m/z* 185.0709 (γ-carbolinone core), at *m/z* 167.0604 (loss of water), and at *m/z* 119.0855 (cumyl moiety). The most abundant fragment was, after cleavage of the cumyl moiety, at *m/z* 293.1648, corresponding to the NBM side chain attached to the γ-carbolinone core. The cleavage of the NBM produced the fragment at *m/z* 197.1648, and the NBM tail structure was detected at *m/z* 109.1012. This fragmentation pattern is consistent with the analytical data provided elsewhere.[14]

The analysis of the four authentic urine samples did not detect the unchanged parent compound, as seen for the majority of SCRAs.

In total, nine phase-I metabolites were detected in the investigated set of authentic urine samples. After cleavage of glucoronides, the metabolic reactions consisted of monohydroxylation, dihydroxylation, *N*-decumylation, and *N*-dealkylation combined with monohydroxylation (Table 2, also showing MAR% for each metabolite).

In Figure 3, the fragmentation patterns of Cumyl-NBMEGACLONE and its metabolites are shown.

With $[M + H]^+$ at *m/z* 427.2380 (+15.9949 u compared with the parent compound), M8 and M9 were detected, being the most abundant metabolites in the authentic urine samples. However, compared with M9, which was chosen as the most abundant (MAR% 100%), M8 showed an MAR% of only 35.1%. Both were identified with characteristic fragment ions at *m/z* 119.0855, at *m/z* 185.0709, and at *m/z* 197.0709, identical to the parent compound, and by a fragment at *m/z* 309.1598. Given the shift of both this latter fragment and the protonated mass, M8 and M9 were deemed products of a monohydroxylation occurring at the NBM group. Additionally, a fragment at *m/z* 449.2199, corresponding to the sodium adduct, and one at *m/z* 291.1492, likely due to the loss of water from the fragment at *m/z* 309.1598, were detected. With minor intensity, further fragments at *m/z* 125.0961 and at *m/z* 107.0855, likely corresponding to the monohydroxylated NBM tail and to the loss of water, were seen in vivo and confirmed by corresponding in vitro metabolites.

M4–M6 presented a molecular ion ($[M + H]^+$) at *m/z* 443.2329 (+31.9898 u compared with the parent compound). The three metabolites were all detected with fragment ions at *m/z* 185.0709 (the unaltered core) and at *m/z* 119.0855 (the cumyl moiety), coupled to the fragment at *m/z* 309.1598, which suggests a monohydroxylation at the NBM group. Additionally, fragments at *m/z* 325.1547 and at *m/z* 307.1441, likely due to loss of water, were noted, so that M4–M6 were deemed products of dihydroxylation, with both biotransformations involving the NBM tail. This was confirmed by the analysis of pHLM, additionally showing a fragment at *m/z* 289.1335, explained by another loss of a water molecule. The sodium adduct ion, at *m/z* 465.2147, was additionally detected in the spectrum of M4–M6.

M1–M3 had a protonated mass at *m/z* 319.1441. The fragmentation pattern for all three metabolites consists of a fragment at *m/z*

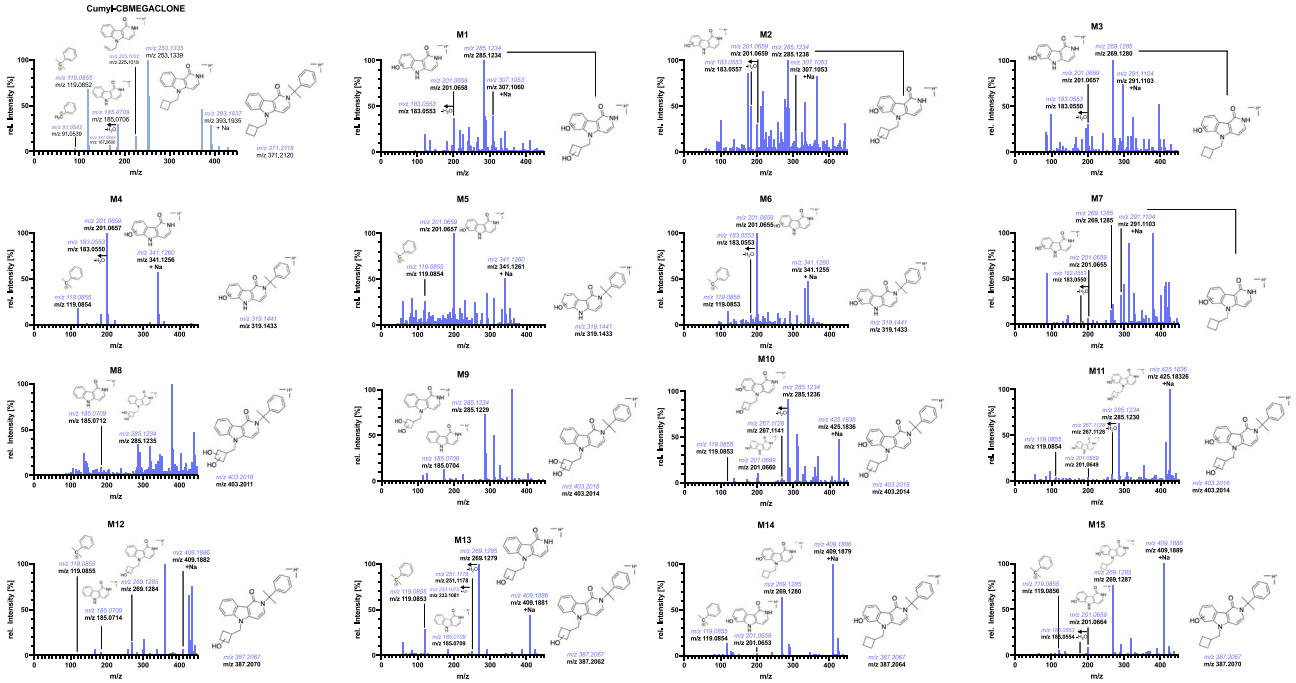

FIGURE 2 Liquid chromatography–quadrupole time-of-flight mass spectrometry spectra of Cumyl-CBMEGACLONE (M00, taken from analysis of the reference standard) and of its urinary metabolites, as observed in authentic urine specimens (broadband collision-induced dissociation data analysis, with background subtraction for minor metabolites). *m/z* is shown as theoretical, colored and in italic, and experimental, bolded in black, just below.

119.0855 and fragments detected at *m/z* 201.0659 and *m/z* 183.0553. The fragment ion at *m/z* 201.0659 (+15.9950 u with respect to the unaltered core at *m/z* 185.0709) indicated a monohydroxylation occurring at the γ-carbolinone core, and the fragment ion at *m/z* 183.0553 can be attributed to the loss of water, as already seen for Cumyl-CBMEGACLONE metabolites. Together, characteristic ions, including one at *m/z* 341.1260 (the sodium adduct), and the protonated mass pointed toward a reaction of *N*-dealkylation coupled to monohydroxylation at the γ-carbolinone core. M1 was third in the ranking position, with an MAR% of 27.8% among all authentic urine samples.

Products of monohydroxylation at the cumyl moiety and at the core structure, without *N*-dealkylation, were not detected in vivo but only by pHLM assay.

Lastly, M7 showed a $[M + H]^+$ at *m/z* 293.1648 and characteristic fragments at *m/z* 185.0709 and *m/z* 167.0604, both suggesting an intact core, and at *m/z* 315.1468. Thus, M7 is considered a product of *N*-decumylation.

An extracted ion chromatogram obtained from one authentic urine sample is shown in Figure S6.

In the pHLM assays, six out of nine in vivo detected metabolites could be confirmed, with the exclusion, as already seen for Cumyl-CBMEGACLONE, of the products of *N*-dealkylation coupled to monohydroxylation. M7, the product of *N*-decumylation, could be confirmed by in vitro analysis. An extracted ion chromatogram from a pHLM assay and spectra of Cumyl-NBMEGACLONE metabolites as obtained from in vitro analysis are shown in Figures S7 and S8, respectively.

3.3 | Cumyl-NBMINACA

Cumyl-NBMINACA ($[M + H]^+$ at *m/z* 388.2383) was not detected in the two authentic urine samples analyzed. By pHLM and blank control, under the applied LC-qToF-MS conditions, Cumyl-NBMINACA eluted at 12.0 min. The fragmentation pattern of the parent compound allowed to detect fragments corresponding to the cumyl moiety, particularly at *m/z* 119.0855 and at *m/z* 91.0542 (loss of water). The indazole core (at *m/z* 145.0396) was identified and, when coupled to the NBM tail structure, was detected at *m/z* 253.1335. The cleavage of the cumyl moiety was further associated to a fragment at *m/z* 270.1601, while the NBM tail structure was detected at *m/z* 109.1012. The fragmentation pattern is shown in Figure 4.

In authentic urine samples, a total of 13 metabolites were detected, and human in vivo metabolic reactions included monohydroxylation, dihydroxylation, and trihydroxylation. Results are shown in Figures 4 and 5 and Table 3.

M8–M13, with $[M + H]^+$ at *m/z* 404.2333, were built by oxidative biotransformation within phase-I metabolism (shift of +15.9950 u compared with the parent compound). They seem to be monohydroxylated at the NBM tail structure, as suggested by their characteristic product ions, which were detected at *m/z* 286.1550 (+15.9949 u compared with the ion at *m/z* 270.1601), at *m/z* 268.1444, likely due to loss of water, at *m/z* 269.1285 (+15.9950 u compared with the fragment at *m/z* 253.1335), and at *m/z* 145.0396 as well as at *m/z* 119.0855, corresponding to the unaltered core and cumyl moiety. Additional fragments were seen at *m/z* 426.2152, consistent with the sodium adduct, and with very low intensity at *m/z*

TABLE 2 Cumyl-NBMEGACLONE human phase-I metabolites detected by liquid chromatography–quadrupole time-of-flight mass spectrometry analysis of four urine samples.

ID	RT (min)	Biotransformation	Ranking position	MAR in vivo (% and (*SD*))	Number of positive samples	Calculated $[M+H]^+$	Formula $[M+H]^+$	Mass error (ppm)	Diagnostic product ions calc. (*m/z*)	Diagnostic product ions formula	Diagnostic product ions mass error (ppm)	In vitro confirmation via pHLM
M00	10.5	–	–	–	–	411.2431	$C_{28}H_{31}N_2O^+$	−1.9	119.0855	$C_9H_{11}^+$	−1.4	–
									185.0709	$C_{11}H_9N_2O^+$	−0.7	
									293.1648	$C_{19}H_{21}N_2O^+$	1.4	
M1	3.9	*N*-dealkylation (NBM) + monoOH (core)	3	27.8% (4.1)	4	319.1441	$C_{20}H_{19}N_2O_2^+$	1.8	201.0659	$C_{11}H_9N_2O_2^+$	1.5	–
									119.0855	$C_9H_{11}^+$	−0.3	
M2	4.1	*N*-dealkylation (NBM) + monoOH (core)	8	3.3% (6.5)	1	319.1441	$C_{20}H_{19}N_2O_2^+$	−0.8	201.0659	$C_{11}H_9N_2O_2^+$	−1.8	–
									119.0855	$C_9H_{11}^+$	−2.9	
M3	4.4	*N*-dealkylation (NBM) + monoOH (core)	5	7.2% (6.2)	3	319.1441	$C_{20}H_{19}N_2O_2^+$	−0.4	201.0659	$C_{11}H_9N_2O_2^+$	1.7	–
									119.0855	$C_9H_{11}^+$	−1.4	
M4	5.1	DiOH (NBM; NBM)	9	0.6% (1.3)	1	443.2329	$C_{28}H_{31}N_2O_3^+$	1.2	309.1598	$C_{19}H_{21}N_2O_2^+$	−2.2	✓
									325.1547	$C_{19}H_{21}N_2O_3^+$	0.1	
M5	5.4	DiOH (NBM; NBM)	4	10.5% (4.7)	4	443.2329	$C_{28}H_{31}N_2O_3^+$	0.9	309.1598	$C_{19}H_{21}N_2O_2^+$	−1.2	✓
									325.1547	$C_{19}H_{21}N_2O_3^+$	−0.6	
M6	5.7	DiOH (NBM; NBM)	6	4.8% (2.7)	4	443.2329	$C_{28}H_{31}N_2O_3^+$	−0.8	309.1598	$C_{19}H_{21}N_2O_2^+$	−1.2	✓
									185.0709	$C_{11}H_9N_2O^+$	−1.5	
M7	7.5	*N*-decumylation	7	4.6% (6.3)	2	293.1648	$C_{19}H_{21}N_2O^+$	−2.2	167.0604	$C_{11}H_7N_2^+$	−3.1	✓
									185.0709	$C_{11}H_9N_2O^+$	−4.1	
M8	7.9	MonoOH (NBM)	2	35.1% (12.5)	4	427.2380	$C_{28}H_{31}N_2O_2^+$	−1.1	309.1598	$C_{19}H_{21}N_2O_2^+$	−1.4	✓
									197.0709	$C_{12}H_9N_2O^+$	0.7	
M9	8.9	MonoOH (NBM)	1	100% (0)	4	427.2380	$C_{28}H_{31}N_2O_2^+$	−1.1	309.1598	$C_{19}H_{21}N_2O_2^+$	−1.6	✓
									197.0709	$C_{12}H_9N_2O^+$	−0.6	

Note: Ranking position is based on the mean MAR%, calculated in relation to the most abundant metabolite peak.

Abbreviations: DiOH, dihydroxylation; MAR, mean area ratio; MonoOH, monohydroxylation; NBM, norbornyl methyl; pHLM, pooled human liver microsome; RT, retention time; *SD*, standard deviation.

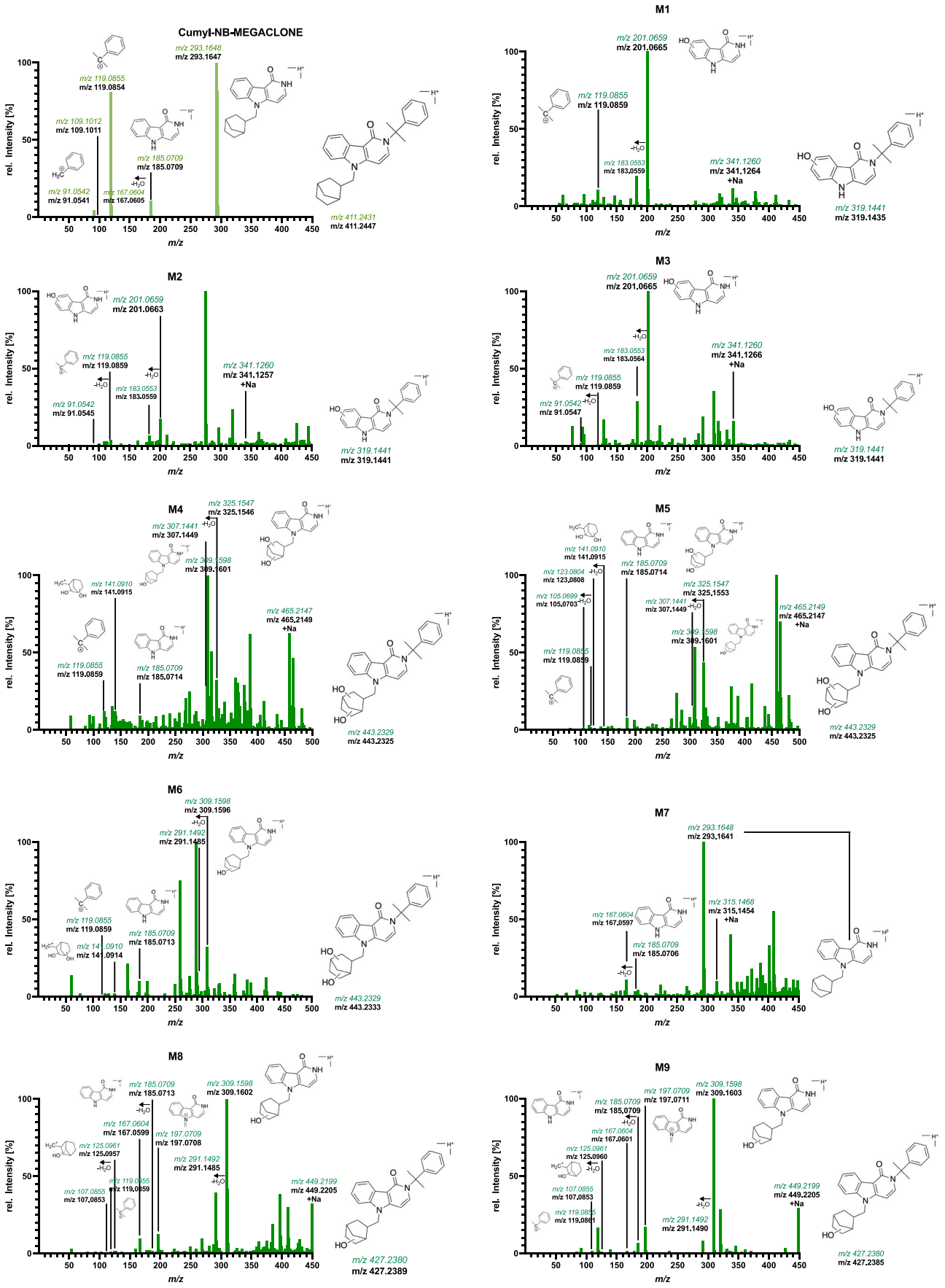

FIGURE 3 Legend on next page.

FIGURE 3 Liquid chromatography–quadrupole time-of-flight mass spectrometry spectra of Cumyl-NBMEGACLONE (M00, taken from analysis of the reference standard) and of its urinary metabolites as observed in authentic urine specimens. *m/z* is shown as theoretical, colored and in italic, and experimental, bolded in black, just below.

125.0961, as well as *m/z* 107.0855, corresponding to the monohydroxylated NBM tail and loss of water. The loss of water molecules, better highlighted in the corresponding in vitro-generated metabolites, allowed to confirm the position of monohydroxylation at the tail. M8–M13 did not rank among the highest abundant metabolites.

No monohydroxylated metabolite at the core or at the cumyl group was detected in vivo.

M5–M7 were detected with $[M + H]^+$ at *m/z* 420.2282 and were probably formed by dihydroxylation, as demonstrated by the shift of +31.9899 u from the parent compound, as well as by the fragmentation pattern. These metabolites, indeed, showed characteristic fragment ions at the unaltered core and at the unaltered cumyl moiety coupled with those at *m/z* 285.1234, *m/z* 267.1128 due to loss of water, at *m/z* 302.1499, after cleavage of the cumyl moiety, and at *m/z* 442.2101, the sodium adduct. The fragmentation pattern suggested that both hydroxylations should be located at the NBM moiety. Among the metabolites detected in vivo, M7 appeared as the most abundant.

M1–M4 were probably built by trihydroxylation, as shown by the protonated mass ($[M + H]^+$) at *m/z* 436.2231. M1–M4 shared with M5–M7 the fragment ions at *m/z* 285.1234, *m/z* 267.1128 due to loss of water, *m/z* 302.1499, after cleavage of the cumyl moiety, and at *m/z* 145.0396, which both pointed toward a dihydroxylation at the tail. Moreover, the characteristic ion at *m/z* 135.0804 could be detected, proving a further hydroxylation of the cumyl moiety, as well as low-intensity fragment ions at *m/z* 141.0910 and at *m/z* 123.0804, corresponding to the dihydroxylated NBM tail and loss of water. Furthermore, the sodium adduct was detected at *m/z* 458.2050. Considering the products of trihydroxylation, M3 and M4 ranked at the second and third places among the authentic urine samples analyzed in this study.

A total of 22 metabolites were identified by analysis of pHLM, providing a confirmation of 9 out of 13 in vivo detected metabolites. Particularly, the in vivo detected metabolites M5–M13, built by monohydroxylation and dihydroxylation, were confirmed in vitro. In these cases, minor fragment ions are not always identified in vivo. In the case of M5–M7, particularly, the in vitro metabolite additionally showed fragment ions at *m/z* 141.0910, at *m/z* 123.0804, and at *m/z* 105.0699 (likely due to loss of water molecules), which is not typical of *N*-oxides but supports dihydroxylation at a nonaromatic substructure, like the tail. The same applies to M8 and M9. Trihydroxylated metabolites M1–M4, on the contrary, were not built by the in vitro assay. In vitro-generated metabolites included further products of monohydroxylation and dihydroxylation, as well as metabolites built by *N*-dealkylation and ketone formation, not confirmed in vivo. M8 and M9, detected in vivo and confirmed in vitro, showed the highest abundance in the pHLM assay but presented an MAR% of 12.6% and 44% in authentic urine samples. The most abundant in vivo metabolite, M7, was low in the pHLM ranking, and M3 (second in the in vivo score) was not confirmed in vitro at all.

In Supporting Information S1, the extracted ion chromatograms of one authentic urine sample (Figure S9) and one pHLM assay (Figure S10), as well as the spectra of the CUmyl-NBMINACA metabolites generated via pHLM (Figure S11), are reported.

3.4 | Urinary biomarkers

The human phase-I metabolism of several SCRAs bearing a cumyl moiety, linked to a γ-carbolinone, indole, or indazole core, has been already reported, possibly leading to metabolites identical to the SCRAs herein analyzed.[9,11,13,20–23]

In our study, the most abundant in vivo detected metabolite of Cumyl-CBMEGACLONE was M13, which was characterized by a monohydroxylation at the CBM residue. This is congruent with previous results for SCRAs bearing a CBM tail, particularly with Cumyl-CBMINACA.[13] Notably, M13 was also the most abundant in vitro metabolite, and this finding is again congruent with the indazole analog of Cumyl-CBMEGACLONE.[13]

By maintaining the CBM tail, M13 allowed a distinction of the consumption of structurally related SCRAs like Cumyl-CHMEGACLONE[11] and Cumyl-NBMEGACLONE. M13 is thus considered a specific urinary biomarker.

M4 ranked second among the analyzed authentic urine samples. However, metabolites built by *N*-dealkylation plus monohydroxylation of Cumyl-CBMEGACLONE, M4–M6, were identical to the products of structurally related SCRAs like Cumyl-CHMEGACLONE, Cumyl-PEGACLONE, and Cumyl-5F-PEGACLONE.[9,11,20] Such overlap was expected for products of *N*-decumylation and *N*-dealkylation, which remove the cumyl moiety and/or the CBM residue and, thus, eliminate characteristic features of the corresponding SCRA. M1–M3 and M7 have not been detected so far in vivo for Cumyl-CHMEGACLONE,[11] but their formation could not be excluded.

Metabolites dihydroxylated at the tail of Cumyl-CBMEGACLONE, like M8 and M9, could be isomeric to the pentanoic acid metabolite formed by human transformation of Cumyl-PEGACLONE and Cumyl-5F-PEGACLONE.[9,20]

A second specific marker is represented by M14, built by monohydroxylation at the core, and the monitoring of this metabolite can be strongly suggested, although it ranked only at the fourth position.

Considering the human phase-I metabolites of Cumyl-NBMEGACLONE, the highest in vivo detected metabolites were represented by M8 and M9, both formed by monohydroxylation at the NBM moiety. Given the fact that these metabolites were characterized by the intact structure of the parent drug, including linked group and tail, M8 and M9 can be considered not only abundant but

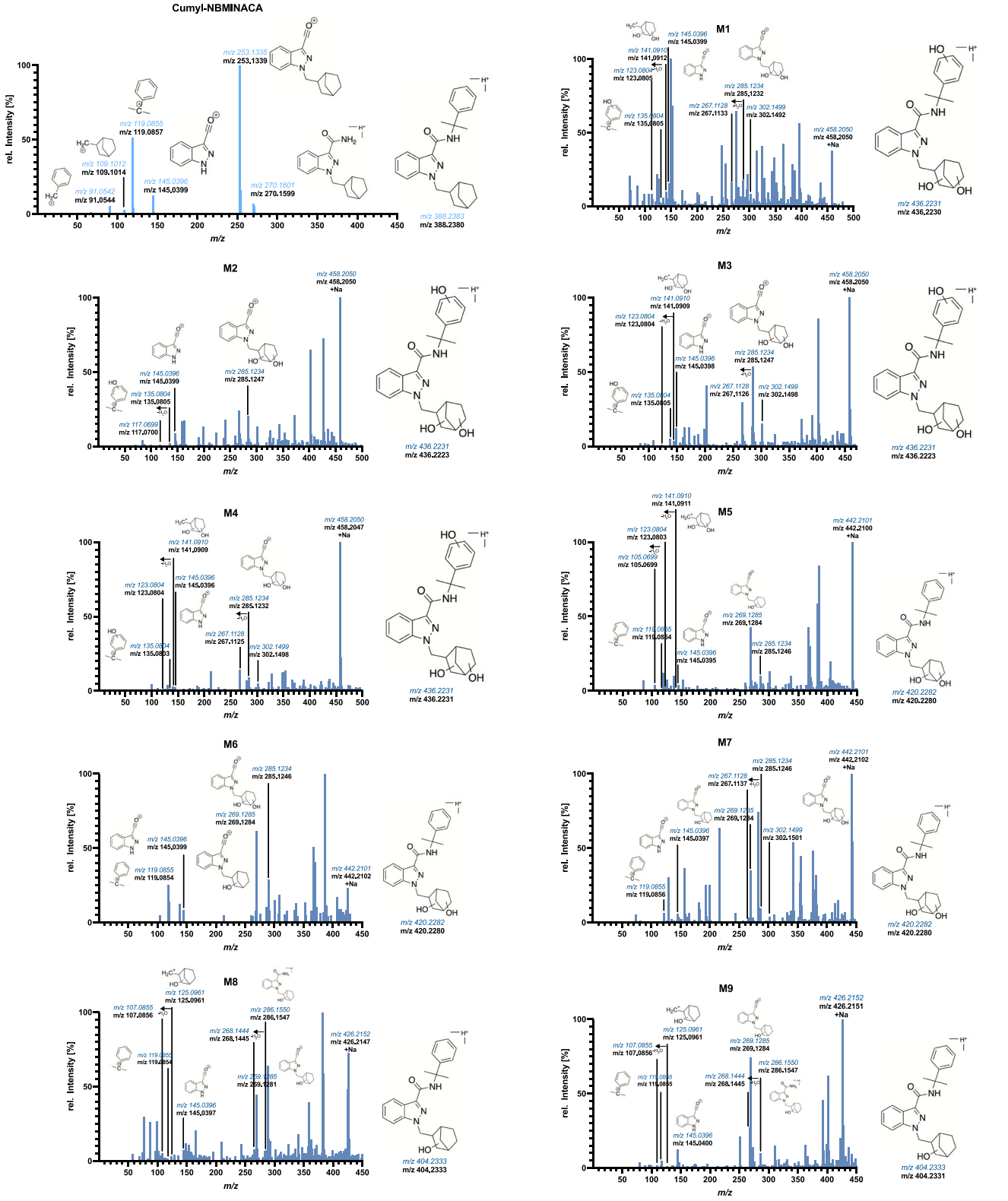

FIGURE 4 Liquid chromatography–quadrupole time-of-flight mass spectrometry spectra of Cumyl-NBMINACA (M00, taken from analysis of the reference standard) and of its urinary metabolites, as observed in authentic urine specimens (broadband collision-induced dissociation data analysis, with background subtraction for minor metabolites), part 1. *m/z* is shown as theoretical, colored and in italic, and experimental, bolded in black, just below.

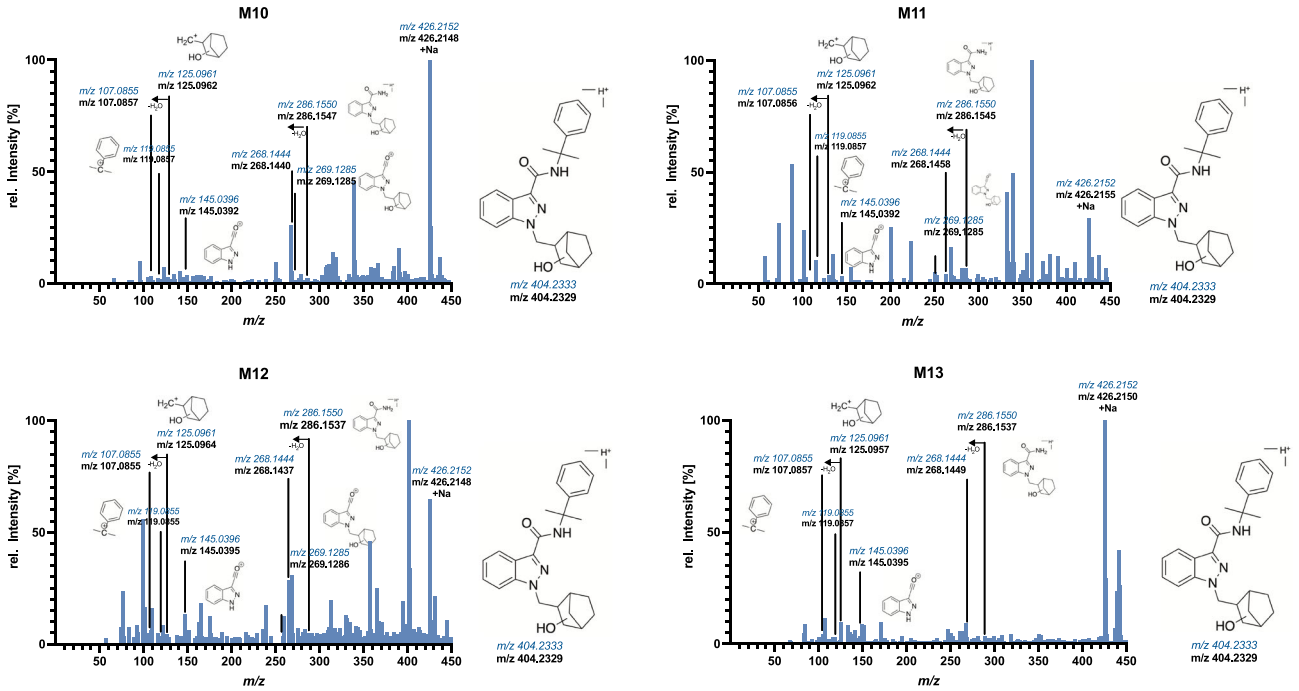

FIGURE 5 Liquid chromatography–quadrupole time-of-flight mass spectrometry spectra of Cumyl-NBMINACA urinary metabolites, as observed in authentic urine specimens (broadband collision-induced dissociation data analysis, with background subtraction for minor metabolites), part 2. *m/z* is shown as theoretical, colored and in italic, and experimental, bolded in black, just below.

also highly specific markers to unambiguously detect the consumption of Cumyl-NBMEGACLONE.

Cumyl-NBMINACA is structurally related to a number of further compounds, including Cumyl-CBMINACA, Cumyl-PINACA, and its analogs (e.g., Cumyl-4Cl-PINACA).[13,21,22] Theoretically, the products of *N*-dealkylation of Cumyl-CBMINACA, coupled or not to monohydroxylation, would be identical to the metabolites of Cumyl-NBMINACA,[13] but this was not seen in the analyzed samples.

In contrast to other structurally related SCRAs carrying a cumyl moiety, for example, Cumyl-PINACA, Cumyl-5F-PINACA,[21] Cumyl-4CN-BINACA,[23] or Cumyl-CBMINACA,[13] none of the metabolites of Cumyl-NBMINACA detected in vivo showed monohydroxylation at the cumyl moiety, and no product of dihydrodiol formation could be detected.

The absence of metabolites formed by monohydroxylation at the indazole core of Cumyl-NBMINACA is consistent with past metabolism studies.[13,24]

Despite the limited number of authentic urine samples explored in this study, all the metabolites detected in vivo retained both the NBM tail and the cumyl moiety, supporting their use as specific markers of Cumyl-NBMINACA consumption.

Given their high abundance, the monitoring of M7 and M3, formed by dihydroxylation at the NBM structure and by an additional hydroxylation at the cumyl moiety, can be suggested, although the analysis of a greater number of authentic urine samples would be needed for confirmation.

Regarding comparisons with the pHLM assays, metabolites of Cumyl-CBMEGACLONE or Cumyl-NBMEGACLONE built by *N*-dealkylation plus monohydroxylation or dihydroxylation and products of trihydroxylation of Cumyl-NBMINACA could not be confirmed by in vitro assays, as expected given the fact that the pHLM has a weak tendency to form metabolites by multiple, complex biotransformation pathways.[25] Past in vitro studies on Cumyl-CHMEGACLONE,[11] but also on structurally unrelated SCRAs, like ADB-BINACA,[26] also did not mention such multiple metabolic reactions products, underlining that in vivo data are essential in order to prevent missing relevant human metabolites.

3.5 | Limitations

Several isomeric metabolites with identical fragment ions but different retention times were detected for the investigated SCRAs.[11,13,19] In order to identify the exact chemical structure of these metabolites, that is, the position of the functional groups introduced, the synthesis of reference material,[27] or the structure elucidation of the isolated metabolites of interest, for example, by NMR spectroscopy, would be required. This was beyond the scope of our study.

As a second limitation, the in vivo MAR% here described was based on the chromatographic peak areas. It might not accurately reflect absolute concentrations, given possible differences in ionization efficiency and matrix effects.[13]

Another major drawback is represented by the fact that it was not always possible to obtain clear spectra from data-independent acquisition, due to limited sample material and the need to concentrate samples.

TABLE 3 Cumyl-NBMINACA human phase-I metabolites detected by liquid chromatography–quadrupole time-of-flight mass spectrometry analysis of two urine samples.

ID	RT (min)	Biotransformation	Ranking position	MAR in vivo (% and (*SD*))	Number of positive samples	Calculated $[M+H]^+$	Formula (M)	Mass error (ppm)	Diagnostic product ions calc. (*m/z*)	Diagnostic product ions formula	Diagnostic product ions mass error (ppm)	In vitro confirmation via pHLM
M00	12	–	–	–	–	388.2383	$C_{25}H_{30}N_3O^+$	0.2	119.0855	$C_9H_{11}^+$	−1.9	–
									145.0396	$C_8H_5N_2O^+$	−1.8	
									253.1335	$C_{16}H_{17}N_2O^+$	−1.6	
M1	3.8	TriOH (cumyl; NBM; NBM)	5	55.1% (2.1)	2	436.2231	$C_{25}H_{30}N_3O_4^+$	0.3	145.0396	$C_8H_5N_2O^+$	−1.4	–
									285.1234	$C_{16}H_{17}N_2O_3^+$	−0.0	
M2	3.9	TriOH (cumyl; NBM; NBM)	7	40.1% (2.9)	2	436.2231	$C_{25}H_{30}N_3O_4^+$	1.7	145.0396	$C_8H_5N_2O^+$	−4.9	–
									285.1234	$C_{16}H_{17}N_2O_3^+$	0.0	
M3	4.1	TriOH (cumyl; NBM; NBM)	2	89.4% (3.0)	2	436.2231	$C_{25}H_{30}N_3O_4^+$	−0.4	145.0396	$C_8H_5N_2O^+$	−2.0	–
									285.1234	$C_{16}H_{17}N_2O_3^+$	−1.1	
M4	4.4	TriOH (cumyl; NBM; NBM)	3	82% (0.2)	2	436.2231	$C_{25}H_{30}N_3O_4^+$	0.3	267.1128	$C_{16}H_{15}N_2O_3^+$	0.3	–
									285.1234	$C_{16}H_{17}N_2O_3^+$	−0.5	
M5	5.8	DiOH (NBM; NBM)	8	38.6% (27.1)	2	420.2282	$C_{25}H_{30}N_3O_3^+$	0.3	269.1285	$C_{16}H_{17}N_2O_2^+$	0.4	✓
									285.1234	$C_{16}H_{17}N_2O_3^+$	0.8	
M6	5.9	DiOH (NBM; NBM)	4	55.3% (11.9)	2	420.2282	$C_{25}H_{30}N_3O_3^+$	4.3	269.1285	$C_{16}H_{17}N_2O_2^+$	0.4	✓
									145.0396	$C_8H_5N_2O^+$	−2.5	
M7	6.2	DiOH (NBM; NBM)	1	100% (0)	2	420.2282	$C_{25}H_{30}N_3O_3^+$	1.4	269.1285	$C_{16}H_{17}N_2O_2^+$	0.0	✓
									145.0396	$C_8H_5N_2O^+$	−0.2	
M8	8.1	MonoOH (NBM)	10	12.6% (16.7)	1	404.2333	$C_{25}H_{30}N_3O_2^+$	−0.2	269.1285	$C_{16}H_{17}N_2O_2^+$	1.4	✓
									145.0396	$C_8H_5N_2O^+$	−2.0	
M9	8.3	MonoOH (NBM)	6	44.4% (1.36)	2	404.2333	$C_{25}H_{30}N_3O_2^+$	0.5	269.1285	$C_{16}H_{17}N_2O_2^+$	0.1	✓
									145.0396	$C_8H_5N_2O^+$	−0.5	
M10	8.6	MonoOH (NBM)	9	34.8% (7.5)	2	404.2333	$C_{25}H_{30}N_3O_2^+$	0.9	268.1444	$C_{16}H_{18}N_3O^+$	0.5	✓
									145.0396	$C_8H_5N_2O^+$	2.7	
M11	9	MonoOH (NBM)	11	10.3% (14.7)	1	404.2333	$C_{25}H_{30}N_3O_2^+$	2.1	269.1285	$C_{16}H_{17}N_2O_2^+$	−0.4	✓
									119.0855	$C_9H_{11}^+$	−1.5	
M12	9.8	MonoOH (NBM)	12	3.9% (5.5)	1	404.2333	$C_{25}H_{30}N_3O_2^+$	0.4	269.1285	$C_{16}H_{17}N_2O_2^+$	3.1	✓
									145.0396	$C_8H_5N_2O^+$	0.9	
M13	10.4	MonoOH (NBM)	13	3.7% (5.2)	1	404.2333	$C_{25}H_{30}N_3O_2^+$	0.4	145.0396	$C_8H_5N_2O^+$	0.6	✓
									119.0855	$C_9H_{11}^+$	−1.5	

Note: Ranking position is based on the mean MAR%, calculated in relation to the most abundant metabolite peak.

Abbreviations: DiOH, dihydroxylation; MAR, mean area ratio; MonoOH, monohydroxylation; NBM, norbornyl methyl; pHLM, pooled human liver microsome; RT, retention time; *SD*, standard deviation; TriOH, trihydroxylation.

The urine sample preparation with β-glucuronidase likely resulted in a lower number of discovered metabolites, in particular regarding phase-II metabolites. However, as routine analysis usually involves a hydrolysis step, we chose by design to detect phase-I metabolites as specific biomarkers to prove the uptake of Cumyl-CBMEGACLONE, Cumyl-NBMEGACLONE, and Cumyl-NBMINACA.

The number of authentic urine samples is rather a strength for Cumyl-CBMEGACLONE and Cumyl-NBMEGACLONE. On the contrary, only two urine samples were available for Cumyl-NBMINACA. This was likely due to the limited prevalence of the compound in Germany (or at least in the samples collected at the University of Freiburg). We are aware that this limited number of samples does not sufficiently account for potential interindividual variability in hepatic drug metabolizing enzyme activity and that these results should be confirmed on a wider casuistry.

4 | CONCLUSIONS

In the present study, the human phase-I metabolism of three SCRAs bearing a cumyl moiety and a CBM or NBM tail is reported, based on LC-qToF-MS data of authentic urine specimens, confirmed by analysis of in vitro pHLM assays. Products of monohydroxylation, dihydroxylation, and trihydroxylation were found to be specific markers of consumption. Particularly, the products of monohydroxylation at the CBM group (M13) and at the core (M14) can be suggested as urinary biomarkers for detecting and monitoring the consumption of Cumyl-CBMEGACLONE. For the forensic diagnosis of the consumption of Cumyl-NBMEGACLONE, M8 and M9, both products of monohydroxylation occurring at the NBM tail, are recommended, as they proved to be highly specific and highly abundant. Urinary biomarkers for the unequivocal documentation of Cumyl-NBMINACA consumption were identified in M7, built by dihydroxylation at the NBM structure, and M3, formed by an additional hydroxylation at the cumyl moiety, although only a limited number of authentic urine samples were available for this compound. The pHLM assay proved to be a valuable tool for metabolite prediction. However, to receive the full picture and identify the most suitable biomarkers, the analysis of authentic samples remains inevitable.

AUTHOR CONTRIBUTIONS

Arianna Giorgetti: Writing—original draft preparation; conceptualization. **Pietro Brunetti:** Formal analysis; resources. **Belal Haschimi:** Formal analysis; resources. **Benedikt Pulver:** Resources. **Jennifer Paola Pascali:** Methodology. **Jan Riedel:** Resources. **Volker Auwärter:** Writing—review & editing; supervision.

CONFLICT OF INTEREST STATEMENT

The authors have nothing to disclose.

FUNDING INFORMATION

The authors declare no funding.

ORCID

Benedikt Pulver https://orcid.org/0000-0002-7772-2111
Volker Auwärter https://orcid.org/0000-0002-1883-2804

REFERENCES

1. European Monitoring Centre for Drugs and Drug Addiction (EMCDDA). *European Drug Report 2023: Trends and Developments* 2023. https://www.emcdda.europa.eu/publications/european-drug-report/2023_en. Accessed February 22, 2024.
2. Auwärter V, Dresen S, Weinmann W, Müller M, Pütz M, Ferreirós N. "Spice" and other herbal blends: harmless incense or cannabinoid designer drugs? *Mass Spectrom*. 2009;44(5):832-837. doi:10.1002/jms.1558
3. Halter S, Haschimi B, Mogler L, Auwärter V. Impact of legislation on NPS markets in Germany—the rise and fall of 5F-ADB. *Drug Test Anal*. 2020;12(6):853-856. doi:10.1002/dta.2786
4. Bowden MJ, Williamson JPB. Cannabinoid compounds. Patent WO2014167530 A 1. 2014.
5. Angerer V, Mogler L, Steitz J-P, et al. Structural characterization and pharmacological evaluation of the new synthetic cannabinoid CUMYL-PEGACLONE. *Drug Test Anal*. 2018;10(3):597-603. doi:10.1002/dta.2237
6. Halter S, Angerer V, Röhrich J, et al. Cumyl-PEGACLONE: a comparatively safe new synthetic cannabinoid receptor agonist entering the NPS market? *Drug Test Anal*. 2019;11(2):347-349. doi:10.1002/dta.2545
7. Halter S, Mogler L, Auwärter V. Quantification of herbal mixtures containing Cumyl-PEGACLONE—is inhomogeneity still an issue? *J Anal Toxicol*. 2020;44(1):81-85. doi:10.1093/jat/bkz028
8. Ernst L, Langer N, Bockelmann A, Salkhordeh E, Beuerle T. Identification and quantification of synthetic cannabinoids in "spice-like" herbal mixtures: update of the German situation in summer 2018. *Forensic Sci Int*. 2019;294:96-102. doi:10.1016/j.forsciint.2018.11.001
9. Mogler L, Halter S, Wilde M, Franz F, Auwärter V. Human phase I metabolism of the novel synthetic cannabinoid 5F-CUMYL-PEGACLONE. *Forensic Toxicol*. 2019;37(1):154-163. doi:10.1007/s11419-018-0447-4
10. Giorgetti A, Mogler L, Halter S, et al. Four cases of death involving the novel synthetic cannabinoid 5F-Cumyl-PEGACLONE. *Forensic Toxicol*. 2020;38(2):314-326. doi:10.1007/s11419-019-00514-w
11. Haschimi B, Giorgetti A, Mogler L, et al. The novel psychoactive substance Cumyl-CH-MEGACLONE: human phase-i metabolism, basic pharmacological characterization and comparison to other synthetic cannabinoid receptor agonists with a γ-carboline-1-one core. *J Anal Toxicol*. 2021;45(3):277-290. doi:10.1093/jat/bkaa065
12. New Psychoactive Substances Act* (Neue-psychoaktive-Stoffe-Gesetz) (NpSG). https://www.bundesgesundheitsministerium.de/service/begriffe-von-a-z/n/npsg.html#:~:text=Das%20NpSG%20ist%20ein%20eigenständiges,Gesundheitsgefahren%20vorausschauend%20und%20effektiver%20begegnet, 2020. Accessed February 22, 2024.
13. Haschimi B, Grafinger KE, Pulver B, et al. New synthetic cannabinoids carrying a cyclobutyl methyl side chain: human phase I metabolism and data on human cannabinoid receptor 1 binding and activation of Cumyl-CBMICA and Cumyl-CBMINACA. *Drug Test Anal*. 2021;13(8):1499-1515. doi:10.1002/dta.3038
14. Pulver B, Riedel J, Schönberger T, et al. Comprehensive structural characterisation of the newly emerged synthetic cannabimimetics Cumyl-BC[2.2.1]HpMeGaClone, Cumyl-BC[2.2.1]HpMINACA, and Cumyl-BC[2.2.1]HpMICA featuring a norbornyl methyl side chain. *Forensic Chem*. 2021;26:100371. doi:10.1016/j.forc.2021.100371
15. European Monitoring Centre for Drugs and Drug Addiction (EMCDDA). *Synthetic Cannabinoids in Europe: A Review*. https://www.

emcdda.europa.eu/publications/rapid-communications/synthetic-cannabinoids-europe-review_en, 2021. Accessed February 22, 2024.
16. Pulver B, Pütz M, Auwärter V, Westphal F, Sebastian H. Synthetic cannabimimetics with cyclobutyl methyl and norbornyl methyl side chains—pharmacological data and legislative implications. *Toxicol Anal Clin* 2022;34(3,Supplement):S156–157. doi:10.1016/j.toxac.2022.06.265, 3, S157.
17. Pulver B, Schönberger T, Weigel D, et al. Structure elucidation of the novel synthetic cannabinoid Cumyl-Tosyl-Indazole-3-Carboxamide (Cumyl-TsINACA) found in illicit products in Germany. *Drug Test Anal*. 2022;14(8):1387-1406. doi:10.1002/dta.3261
18. Pulver B, Fischmann S, Westphal F, et al. The ADEBAR project: European and international provision of analytical data from structure elucidation and analytical characterization of NPS. *Drug Test Anal*. 2022;14(8):1491-1502. doi:10.1002/dta.3280
19. Giorgetti A, Brunetti P, Haschimi B, Busardò FP, Pelotti S, Auwärter V. Human phase-I metabolism and prevalence of two synthetic cannabinoids bearing an ethyl ester moiety: 5F-EDMB-PICA and EDMB-PINACA. *Drug Test Anal*. 2023;15(3):299-313. doi:10.1002/dta.3405
20. Mogler L, Wilde M, Huppertz LM, Weinfurtner G, Franz F, Auwärter V. Phase I metabolism of the recently emerged synthetic cannabinoid CUMYL-PEGACLONE and detection in human urine samples. *Drug Test Anal*. 2018;10(5):886-891. doi:10.1002/dta.2352
21. Angerer V, Franz F, Moosmann B, Bisel P, Auwärter V. 5F-Cumyl-PINACA in 'e-liquids' for electronic cigarettes: comprehensive characterization of a new type of synthetic cannabinoid in a trendy product including investigations on the in vitro and in vivo phase I metabolism of 5F-Cumyl-PINACA and its non-fluorinated analog Cumyl-PINACA. *Forensic Toxicol*. 2019;37(1):186-196. doi:10.1007/s11419-018-0451-8
22. Stalberga D, Ingvarsson S, Bessa G, et al. Metabolism studies of 4′Cl-CUMYL-PINACA, 4′F-CUMYL-5F-PINACA and 4′F-CUMYL-5F-PICA using human hepatocytes and LC-QTOF-MS analysis. *Basic Clin Pharmacol Toxicol*. 2023;132(3):263-280. doi:10.1111/bcpt.13829
23. Åstrand A, Vikingsson S, Lindstedt D, et al. Metabolism study for CUMYL-4CN-BINACA in human hepatocytes and authentic urine specimens: free cyanide is formed during the main metabolic pathway. *Drug Test Anal*. 2018;10(8):1270-1279. doi:10.1002/dta.2373
24. Franz F, Jechle H, Wilde M, et al. Structure-metabolism relationships of valine and tert-leucine-derived synthetic cannabinoid receptor agonists: a systematic comparison of the in vitro phase I metabolism using pooled human liver microsomes and high-resolution mass spectrometry. *Forensic Toxicol*. 2019;37(2):316-329. doi:10.1007/s11419-018-00462-x
25. Giorgetti A, Zschiesche A, Groth O, et al. ADB-HEXINACA—a novel synthetic cannabinoid with a hexyl substituent: phase I metabolism in authentic urine samples, a case report and prevalence on the German market. *Drug Test Anal*. 2024;1-16. doi:10.1002/dta.3657
26. Sia CH, Wang Z, Goh EML, et al. Urinary metabolite biomarkers for the detection of synthetic cannabinoid ADB-BUTINACA abuse. *Clin Chem*. 2021;67(11):1534-1544. doi:10.1093/clinchem/hvab134
27. Baginski S, Rautio T, Nisbet L, et al. The metabolic profile of the synthetic cannabinoid receptor agonist ADB-HEXINACA using human hepatocytes, LC-QTOF-MS and synthesized reference standards. *J Anal Toxicol*. 2023;00(9):1-8. doi:10.1093/jat/bkad065

SUPPORTING INFORMATION

Additional supporting information can be found online in the Supporting Information section at the end of this article.

How to cite this article: Giorgetti A, Brunetti P, Haschimi B, et al. Human phase-I metabolism of three synthetic cannabinoids bearing a cumyl moiety and a cyclobutyl methyl or norbornyl methyl tail: Cumyl-CBMEGACLONE, Cumyl-NBMEGACLONE, and Cumyl-NBMINACA. *Drug Test Anal*. 2025;17(6):882-896. doi:10.1002/dta.3791